Layered Nickel Oxide-Based Cathodes for Lithium Cells:

Analysis of Performance Loss Mechanisms

Marie Kerlau, Jeffrey A. Reimer, and Elton J. Cairns
Lawrence Berkeley National Laboratory, and
University of California, Berkeley 94720

Abstract

Spectroscopic and electrochemical diagnostic measurements are reported for the cell components of a Generation 2 (Gen 2) Li-Ion cell from the US Department of Energy's Advanced Technology Development (ATD) project. The cells are composed of $LiNi_{0.8}Co_{0.15}Al_{0.05}O_2$ positive electrodes (cathode), carbon graphite anodes and electrolyte consisting of 1.2 M $LiPF_6$ in EC:EMC 3:7. Fluorophosphates were observed by ^{19}F and ^{31}P NMR in the electrolyte obtained from a Gen 2 cell aged 72 weeks at 45°C and presenting 50 % power fade. These electrolyte decomposition products were also observed by ^{31}P solid-state NMR on the surface of the cathode of the same cell. Samples were cut from the aged cathode from the original cell, subjected to different treatments (ultrasonic washing in anhydrous DMC, pressing, ultrasonic washing *and* pressing), and subsequently reassembled into small lab cells for electrochemical characterization. These treatments recovered the capacity of the electrodes to within a few percent of the original value, with the most improvement being obtained with the washed and pressed cathode. The impedance of the cathodes was also lowered after the ultrasonic washing and pressing treatments. Electron microscopy revealed that the ultrasonic washing of the aged Gen 2 cathode material resulted in the removal of small particles covering the surface of the active cathode. These findings are interpreted in terms of a model whereby capacity loss, and thus power capability, is restored by removing the fluorophosphate deposit and restoring electronic contact to the active cathode material.

1. Introduction

Layered nickel-oxide-based active materials are among the most widely used cathodes in commercial lithium ion cells because they exhibit high specific energy and specific power[1]. As part of the US Department of Energy's Advanced Technology Development (ATD) project, so-called Generation 2 (Gen 2) cells are under investigation as part of a long-range plan to develop batteries for hybrid electric vehicle (HEV) applications. Recent research on the cathode material in these cells, $LiNi_{0.8}Co_{0.15}Al_{0.05}O_2$, has shown that cell performance loss is determined largely by the cycling properties of the cathode[2]. A detailed investigation into the mechanical and chemical processes leading to power and capacity loss as a result of cycling or storage is expected to provide useful information for the design of long-lived cells.

The present study reports the results of NMR measurements performed on cell components obtained from a Gen 2 cell that had been aged at 60% state-of-charge and 45˚C for 72 weeks, and had lost 50% of its power capability delivered under the HPPC tests[3]. Samples harvested from the cathode of the aged cell have also been subjected to galvanostatic cycling, Electrochemical Impedance Spectroscopy (EIS), and scanning electron microscopy (SEM), with the intent of understanding the failure mechanisms of the Gen 2 cathode. Taken together, these data suggest that the capacity fade of a Gen 2 cell is attributed to the accumulation of a film of electrolyte decomposition products on the surface of the cathode particles, causing particle isolation and increased impedance at the cathode/electrolyte interface. Removal of the film and reestablishment of particle contact restores almost all of the lost capacity, and dramatically reduces the cathode impedance. We did not investigate the formation of electrolyte reaction products on the anode side. Cell impedance rise is predominantly attributed to the positive electrode; therefore, we focused our work on this electrode.

2. Experimental Equipment and Procedures

The ATD Gen 2 calendar-life cells were cycled and aged at the Argonne National Laboratory (ANL). Characterizations were performed in accordance with the PNGV Battery Test Manual[3]. The profile consisted of constant current discharge and regen pulses with interspersed rest periods centered around 60 % SOC. A $3C_1$ discharge current

(i.e., 3 A) was used. The cumulative length of a single profile is 120 s and constitutes one cycle. This cycle is repeated once every 24 h during life testing, but is interrupted every 28 days (4 weeks) for reference performance tests (RPTs) which are used to characterize changes in capacity, resistance and power. Capacity fade was determined by a $C_1/1$ and a $C_1/25$ capacity tests in the voltage range 3.0 to 4.1 V. Power fade was characterized by a low-current HPPC test. It consisted of a constant-current discharge at a $5C_1$ rate (i.e., 5 A) and regen pulse performed at 75 % of the discharge rate (i.e., 3.75 A). The HPPC test was performed in the voltage range 3.0 to 4.1 V. At the completion of testing, cells were provided for post-test analysis to Lawrence Berkeley National Lab (LBNL).

All cathode and electrolyte materials were harvested from a Gen 2 cell (50 % power fade after 72 weeks of storage at 45˚C and 60% state-of-charge) by disassembly. The electrolyte was obtained by centrifugation of the cell innards and was originally comprised of 1.2 M $LiPF_6$ in EC:EMC 3:7.

Fluorine-19 and phosphorus-31 1D and 2D NMR spectra were obtained on a Bruker AVQ-400 spectrometer operating at a frequency of 400 MHz and on a Bruker AV-500 spectrometer operating at a frequency of 500 MHz, respectively, with a reference of $CFCl_3$ (^{19}F) and 85 % H_3PO_4 (^{31}P). Solid-state ^{31}P NMR experiments were also performed on the Gen 2 cathode material using a spectrometer operating at a frequency of 65 MHz.

The charge and discharge characteristics of the cathode from the aged cell were examined in freshly assembled Swagelok cells using 1 cm^2 samples of the original cathode. The new cells were comprised of the $LiNi_{0.8}Co_{0.15}Al_{0.05}O_2$ cathode harvested from the aged cell, a lithium metal anode, and a separator (Celgard 2300). The electrolyte solution was 1M $LiPF_6$ in 1:1 mixture (by weight) of ethylene carbonate (EC) and diethyl carbonate (DEC). Three 1 cm^2 samples of the aged cathode were subjected to different treatments (washing the electrode ultrasonically in anhydrous DMC, pressing the electrode in a hydraulic press to reduce its thickness by 15% (1 ton/cm^2), or both ultrasonically washing in DMC *and* pressing), and subsequently reassembled into Swagelok test cells for electrochemical characterization. These cells were then galvanostatically cycled between 2.5 and 4.2 V at the C/20 rate (0.057 mA cm^{-2}).

Electrochemical Impedance Spectroscopy (EIS) measurements were performed using a Solartron SI 1286 Electrochemical Interface and a SI 1260 Impedance/Gain-Phase Analyzer, controlled by Zplot software. The measurements were carried out at open circuit voltage (OCV) with an ac oscillation of 10 mV over the frequency range from 100 kHz to 1 mHz.

The morphology of the Gen2 cathodes before and after ultrasonic washing in DMC was monitored with a Field Emission Scanning Electron Microscope (JEOL JSM-6340F) operating at 5 kV.

3. Results and discussion

Figures 1(a) and 1(b) present the ^{19}F and ^{31}P NMR spectra obtained from the electrolyte of the Gen 2 cell, respectively. The ^{19}F NMR spectrum exhibits a doublet at –73.18 ppm, and is assigned to PF_6^-, consistent with data presented in other studies[5,6]. Fluorophosphate species were also observed in the electrolyte, as evidenced by observation of peaks in the chemical shift range –78.0 ppm to –88.0 ppm, as discussed below. The very small peaks observed at -70.95 and -75.43 ppm are instrumental artifacts. The ^{31}P NMR spectrum exhibits a septet at –145.88 ppm corresponding to PF_6^-, as reported elsewhere[7-9]. The fluorophosphates are observed in the chemical range of -5.0 to –30.0 ppm, in accordance with bibliographic data[5-12].

To resolve the complex resonance assignments related to the electrolyte decomposition products, the one-bond couplings between fluorine/phosphorus nuclei have been investigated by the HMBC (heteronuclear multiple bond correlation) experiment. Figure 2 shows the 2D HMBC spectrum depicting fluorine resonances ranging from –78.0 to –88.0 ppm correlated to the phosphorus resonances ranging from –5.0 to –30.0 ppm. The ^{31}P NMR spectrum plotted on the left of the graph has been acquired in fluorine non-decoupling mode, thus the ^{19}F-^{31}P correlated peaks appear in the middle of the ^{31}P multiplets. The observed species, also reported in other works[4-7], correspond to mono- ($OPF(OR)_2$) and difluorophospates ($OPF_2(OR)$) (with R = H, alkyl group), thereby indicating the relative instability of $LiPF_6$ in EC:EMC under the cell testing conditions (60 % SOC, 45C). Five main doublets are observed in the ^{19}F

spectrum and they are assigned to one triplet and four doublets in the ^{31}P NMR spectrum, as shown in Table 1. The ^{19}F doublet at –83.66 ppm (J = 917 Hz) related to the ^{31}P triplet at –20.75 ppm (J = 927 Hz) is assigned to difluorophosphate $OPF_2(OEt)$. The four other main ^{19}F doublets related to the ^{31}P doublets in the region –10.0 to –12.0 ppm are assigned to monofluorophosphates ($OPF_2(OR)_2$). Other correlated doublets with smaller intensities are also observed showing the formation of many phosphate species, especially in the region –10.0 to –12.0 ppm of the ^{31}P spectrum. The substitution of the fluorine atoms bonded to the phosphorus for R groups with different electronegativities would account for this distribution of chemical shifts.

Recent studies have focused on the role of $LiPF_6$-based electrolyte reactivity in the performance of Li-ion battery systems[13-18]. It is known that mixtures of $LiPF_6$ and alkyl carbonates such as ethylene carbonate (EC), dimethylcarbonate (DMC), diethylcarbonate (DEC) and ethylmethylcarbonate (EMC) have poor thermal stability. As reported by Sloop et al.[13], $LiPF_6$ is in equilibrium with solid LiF and PF_5 gas:

$$LiPF_6\,(s) \Leftrightarrow LiF\,(s) + PF_5\,(g)\,. \qquad (1)$$

PF_5 is a strong Lewis acid and therefore reacts readily with the solvents to form decomposition products even at relatively low temperature (45˚C) as demonstrated in this work. Furthermore, in electrolyte solutions HF formation can arise from trace amounts of moisture[16] according to:

$$PF_5\,(g) + H_2O\,(l) \Leftrightarrow 2\,HF\,(g) + OPF_3\,(g) \qquad (2)$$

The substitution of the fluorine atoms in the phosphorus oxyfluoride (OPF_3) compound gives rise to the formation of mono and difluorophosphate species, as observed herein by ^{19}F and ^{31}P NMR.

The fluorophosphate decomposition products and the $LiPF_6$ salt are also present on the surface of the electrode obtained from the aged cell, as evidenced by the ^{31}P NMR spectrum (Fig. 3). It is thus clear that the electrolyte decomposition products can interact

with the electrode particles. A ^{31}P NMR spectrum obtained from an ultrasonically washed cathode (DMC) exhibited no phosphate peaks.

The cycling performance of untreated and treated $LiNi_{0.8}Co_{0.15}Al_{0.05}O_2$ electrodes obtained from the aged Gen 2 cell are shown in Fig. 4. The discharge capacity of a fresh cell, also shown in the plot, is 180 mAh g^{-1}. An initial discharge capacity of 106 mAh g^{-1} is found for the untreated electrode sample. The different treatments improved the capability of the cells, with the greatest improvement being obtained from the washed *and* pressed cathode. In this case, the discharge capacity from the freshly washed and pressed cell was 173 mAh g^{-1}. We surmise that washing removes material from the electrode surface and the pressing re-establishes contact between the particles of active material. The accumulation of the electrolyte decomposition products could be the cause-of particle isolation, thereby resulting in the loss of capacity and power capability.

The EIS data derived from three cells assembled with untreated, pressed, and washed and pressed electrode samples are shown in Fig. 5. For the treated electrodes, two semi-circles and a diffusion straight line appeared, consistent with other studies of $LiNi_{0.8}Co_{0.2}O_2$ electrodes[19-21]. The semi-circle at high frequency indicates the solid-state interface layer resistance and the second semi-circle at medium frequency represents charge transfer resistance at the $LiNi_{0.8}Co_{0.15}Al_{0.05}O_2$ electrode surface. The straight sloping line is due to the diffusion process of lithium ions at the interface between the active material particles and electrolyte. The various treatments of the electrodes drastically decreased the impedance of the cells at low frequency. Moreover, the charge transfer resistance is much smaller in the case of the washed electrode. For the untreated electrode, the semi-circle at medium frequency was not observed due to a very high charge transfer resistance and the balance of the impedance spectrum appears as a straight line. This might be due to the presence of the electrolyte reaction products at the electrode surface, such as those observed by ^{31}P NMR.

We ran control experiments to gauge the pressing effect on the capacity of a freshly made (in our laboratory, not by the supplier; fresh electrodes from the supplier are not available) positive electrode. The pressed electrode (1 ton/cm^2) exhibited a capacity

10 % higher than the capacity of the untreated fresh electrode. The pressing probably improved the interparticle contact and thus the conductivity of the electrode. For the aged samples, the capacity was improved by 30 %. Therefore, the capacity data are slightly different than the data for the electrodes of the cells aged at ANL.

Scanning electron microscopy pictures of unwashed and washed $LiNi_{0.8}Co_{0.15}Al_{0.05}O_2$ cathodes obtained from the cell aged 72 weeks at 45˚C are shown in Figures 6(a) and 6(b), respectively. In the case of the unwashed electrode, particles are clearly evident on the surface of the oxide, as well as on the carbon black and graphite particles. In contrast, the washed cathode exhibited clean surfaces. We conclude that the ultrasonic washing in DMC removes the deposit formed on the surface of the electrode, consistent with the results presented above. The removal of this layer on the active material particles could explain the restoration of the cell capacity as well as the decrease of cell impedance. The formation of this insulating thin layer on the electrode surface is most likely to result from the accumulation of fluorophosphate species from the electrolyte.

4. Conclusions

In this study the failure mechanisms of a Gen 2 cell aged 72 weeks at 45˚C and presenting 50 % of power fade were investigated. The composition of the electrolyte of a Gen 2 cell was investigated by ^{19}F and ^{31}P NMR to probe its stability under the cell testing conditions. The surface of the $LiNi_{0.8}Co_{0.15}Al_{0.05}O_2$ cathode obtained from the same cell was also studied by ^{31}P NMR. Three different treatments were carried out on the cathode before measuring its electrochemical properties to examine the effect of mechanical and contact issues. The initial discharge capacity of a washed and pressed electrode was 65 % higher than that of an untreated electrode, and nearly equal to the original capacity of the electrode. Furthermore, the AC impedance of the washed and pressed electrode was much lower than that of the untreated electrode. The morphologies of an untreated and a washed cathode were different since the formation of a film is observed on the untreated electrode, and is absent from the washed electrode. The capacity fade of a Gen 2 cell is thus attributed to the accumulation of a film of electrolyte

decomposition products on the surface of the cathode particles, causing particle isolation and increased impedance at the cathode/electrolyte interface. Removal of the film and reestablishment of particle contact restored almost all of the lost capacity, and dramatically reduced the cathode impedance.

Acknowledgement

We express our appreciation to the ATD team members at Argonne National Laboratory for providing the cell studied in this investigation.

This work was supported by the Assistant Secretary for Energy Efficiency and Renewable Energy, Office of FreedomCAR and Vehicle Technologies of the U.S. Department of Energy under Contract No. DE-AC03-76SF00098.

We are also thankful to Dr. Herman van Halbeek at the NMR Facility of UC Berkeley for his help in performing the 2D HMBC NMR experiment.

References

1. X. Zhang, P.N. Ross, R. Kostecki, F. Kong, S. Sloop, J.B. Kerr, K.A. Striebel, E.J. Cairns, F. McLarnon, *J. Electrochem. Soc.*, **148**, A463 (2001).

2. D Abraham, ATD review meeting, January 14-15, 2004, Lawrence Berkeley National Laboratory.

3. PNGV battery test manual, INEEL, DOE/ID-10597, Revision 3, 2001.

4. J.R. Macdonald, "Impedance Spectroscopy – Emphasizing Solid Materials and Systems", John Wiley & Sons, New York, 1987.

5. J. Stephen Hartman, James A.W Shoemaker, Alex F. Jansen, Paul J. Ragogna, W.R. Rick Szerminski, Journal of Fluorine Chemistry **119** (2003) 125-139.

6. S. Berger et al., NMR Spectroscopy of the Non-Metallic Elements, Wiley, Chichester, 1997.

7. G.S. Reddy, R. Schmutzler, Z. Naturforsch. **25 B** (1970) 1199.

8. K.O. Christie, D.A. Dixon, G. J. Schrobilgen, W.W. Wilson, J. Am. Chem. Soc. **119** (1997) 3978.

9. M. Forsyth, M.E. Smith, Synthetic Metals **55-57** (1993) 714-719.

10. N. Yoza, S. Nakashima, N. Ueda, T. Miyajima, T. Nakamura, P. Vast, J. Chromatogr. A **664** (1994) 111-116.

11. B. Ravdel, K.M. Abraham, R. Gitzendanner, J. DiCarlo, B. Lucht, C. Campion, Journal of Power Sources **119-121** (2003) 805-810.

12. J.S. Gnanaraj, E. Zinigrad, L. Asraf, M. Sprecher, H.E. Gottlieb, w. Geissler, M. Schmidt, D. Aurbach, Electrochemistry Communications **5** (2003) 946-951.

13. S.E. Sloop, J.B. Kerr, K. Kinoshita, Journal of Power Sources **119-121** (2003) 330-337.

14. J. S. Gnanaraj, E. Zinigrad, L. Asraf, H.E. Gottlib, M. Sprecher, M. Schmidt, W. Geissler, D. Aurbach, Journal of the Electrochemical Society **150** (11) A1533-A1537 (2003).

15. B. Ravdel, K.M. Abraham, R. Gitzendanner, J. DiCarlo, B. Lucht, C. Campion, Journal of Power Sources **119-121** (2003) 805-810.

16. C.L. Campion, W. Li, W.B. Euler, B.L. Lucht, B. Ravdel, J.F. DiCarlo, R. Gitzendanner, K.M. Abraham, Electrochemical and Solid-State Letters **7** (7) A194-A197 (2004).

17. S. Laruelle, S. Pilard, P. Guenot, S. Grugeon, J-M. Tarascon, Journal of Electrochemical Society, **151** (8), A1202-A1209 (2004).

18. G.G. Botte, R.E. White, Z. Zhang, Journal of Power Sources **97-98,** 570-575 (2001).

19. M.D. Levi, K. Gamolsky, D. Aurbach, U. Heider, R. Oesten, Electrochimica Acta **45,** 1781-1789 (2000).

20. G. Ting-Kuo Fey, Zai-Xian Weng, Jian-Ging Chen, T. Prem Kumar, Materials Chemistry and Physics **82,** 5-15 (2003).

21. H. Liu, Z. Zhang, Z. Gong, Y. Yang, Solid State Ionics **166,** 317-325 (2004).

Figure Captions

Figure 1: (a) ^{19}F and (b) ^{31}P NMR spectra of the electrolyte taken from a Gen 2 cell aged at 45C for 72 weeks.

Figure 2: 2D HMBC spectrum showing one-bond coupling between fluorine and phosphorus in the electrolyte decomposition products.

Figure 3: ^{31}P NMR spectrum of a cathode of a Gen 2 cell aged 72 weeks at 45°C and presenting 50 % power fade.

Figure 4: Capacity of $LiNi_{0.8}Co_{0.15}Al_{0.05}O_2$ cathode samples subjected to treatments described in the text.

Figure 5: Nyquist plots of Swagelok cells assembled with $LiNi_{0.8}Co_{0.15}Al_{0.05}O_2$ positive electrodes in the discharged state.

Figure 6: SEM images of $LiNi_{0.8}Co_{0.15}Al_{0.05}O_2$ cathodes before (a) and (b) after washing in DMC.

Table

^{19}F multiplets	^{31}P multiplets
-79.72 ppm, doublet, J_{P-F} = 921 Hz	-11.27 ppm, doublet, J_{P-F} = 907 Hz
-79.90 ppm, doublet, J_{P-F} = 908 Hz	-11.49 ppm, doublet, J_{P-F} = 913 Hz
-82.25 ppm, doublet, J_{P-F} = 960 Hz	-11.78 ppm, doublet, J_{P-F} = 959 Hz
-83.66 ppm, doublet, J_{P-F} = 917 Hz	-20.75 ppm, triplet, J_{P-F} = 927 Hz
-84.58 ppm, doublet, J_{P-F} = 958 Hz	-10.94 ppm, doublet, J_{P-F} = 922 Hz

Table 1: Chemical shifts and coupling constants of the correlated ^{19}F and ^{31}P multiplets observed in the 2D HMBC spectrum.

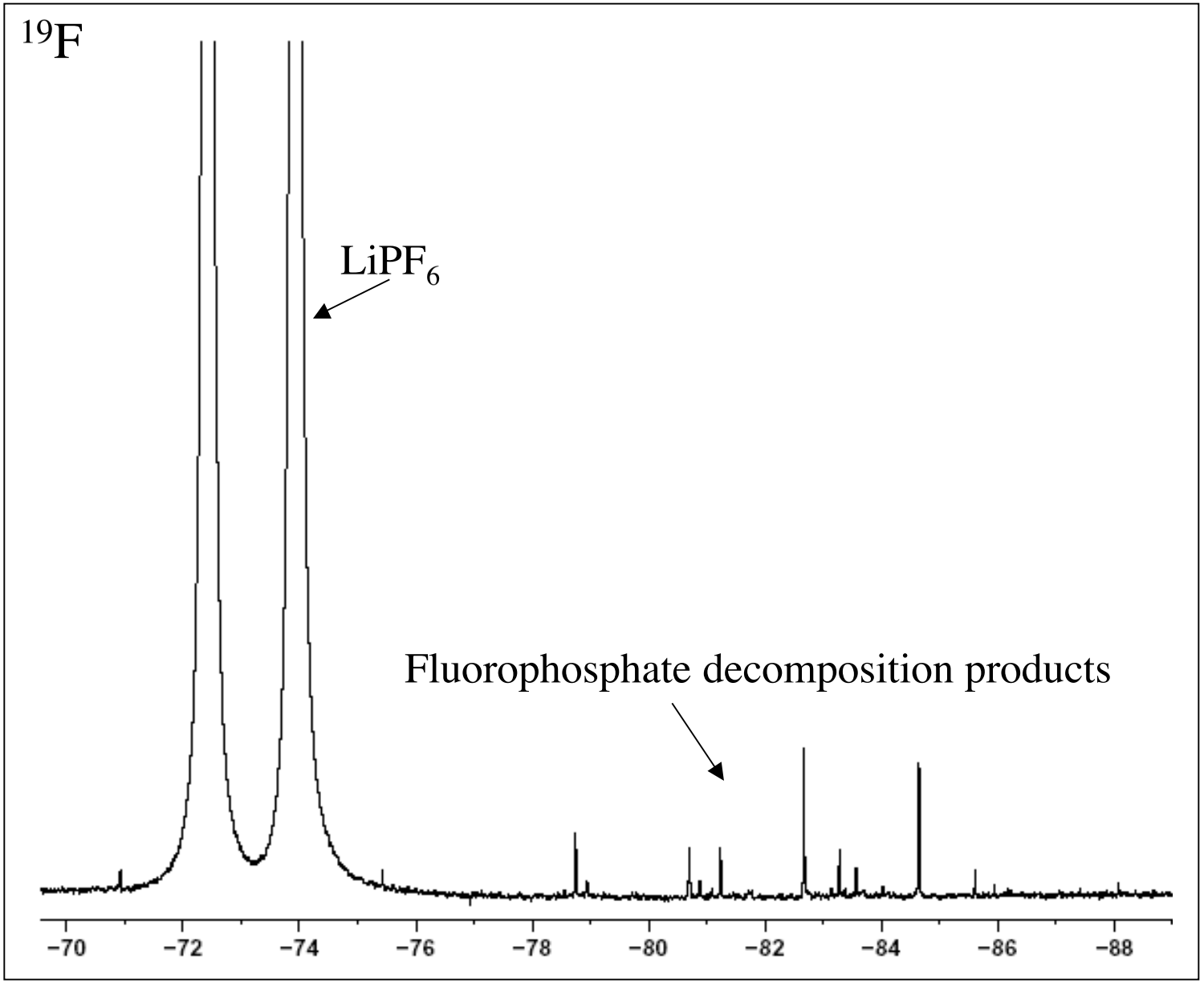
19F
LiPF6
Fluorophosphate decomposition products
−70
−72
−74
−76
−78
−80
−82
−84
−86
−88

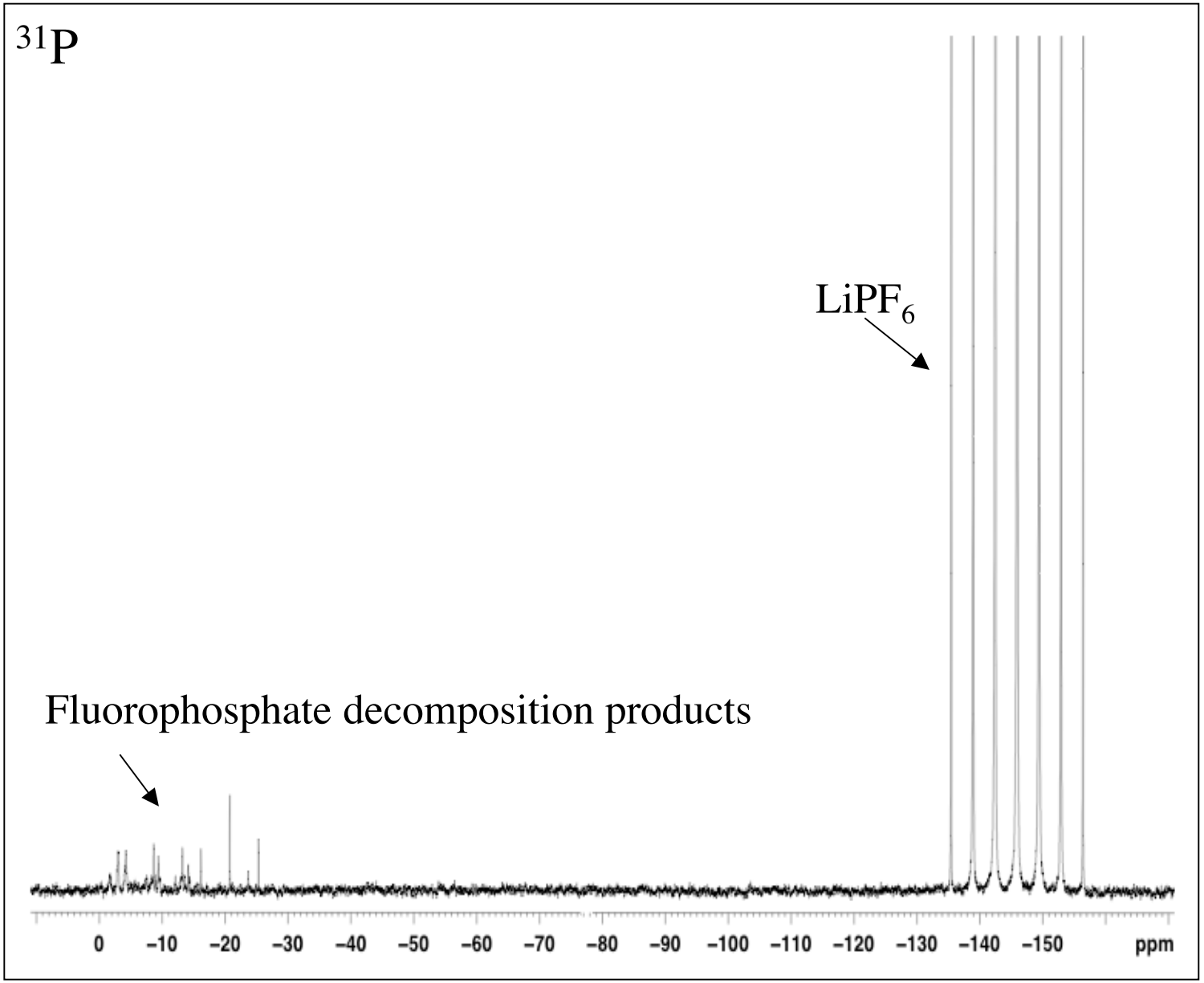
^{31}P
LiPF$_6$
Fluorophosphate decomposition products
0
−10
−20
−30
−40
−50
−60
−70
−80
−90
−100
−110
−120
−130
−140
−150
ppm

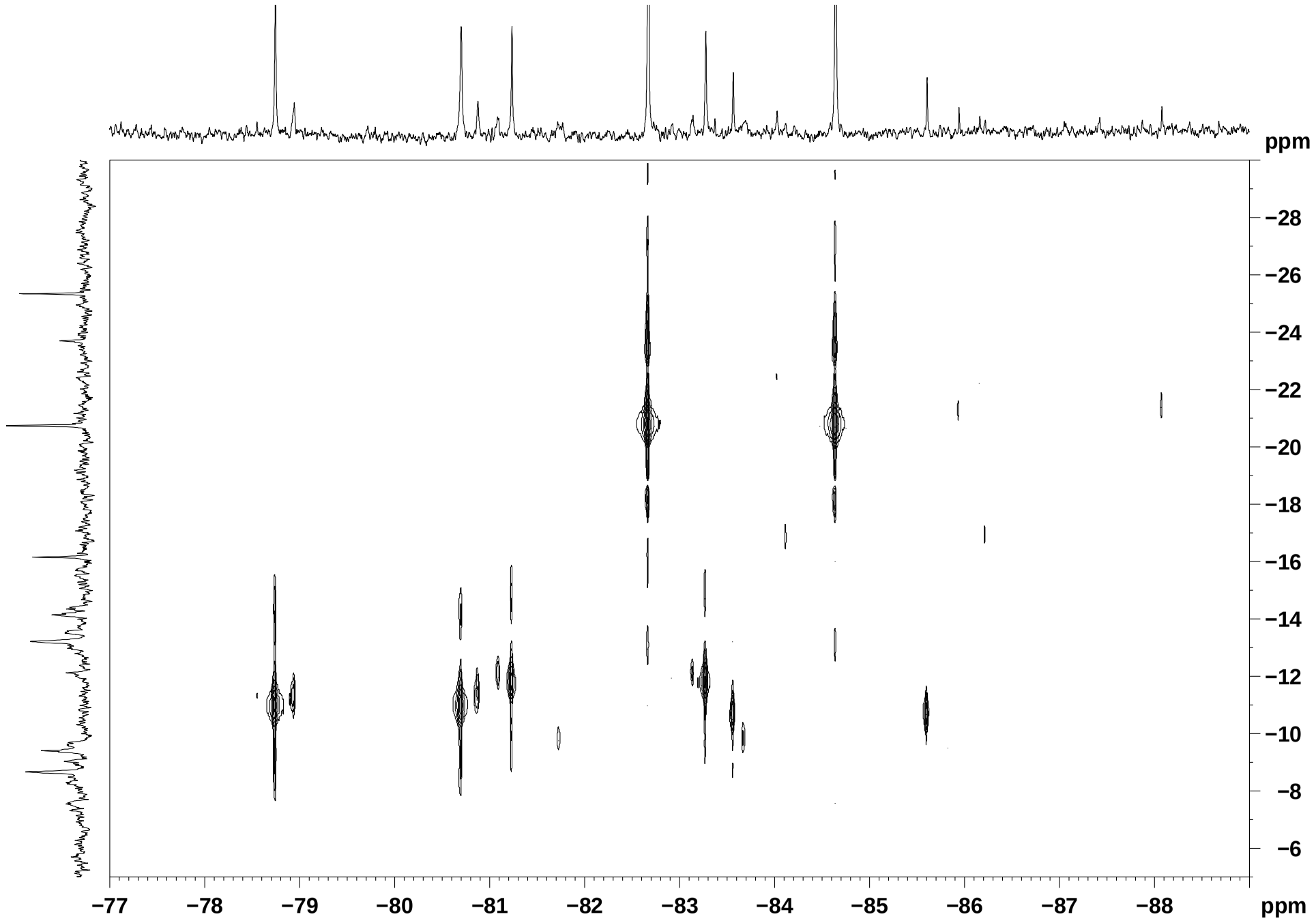
ppm
−28
−26
−24
−22
−20
−18
−16
−14
−12
−10
−8
−6
−77
−78
−79
−80
−81
−82
−83
−84
−85
−86
−87
−88
ppm

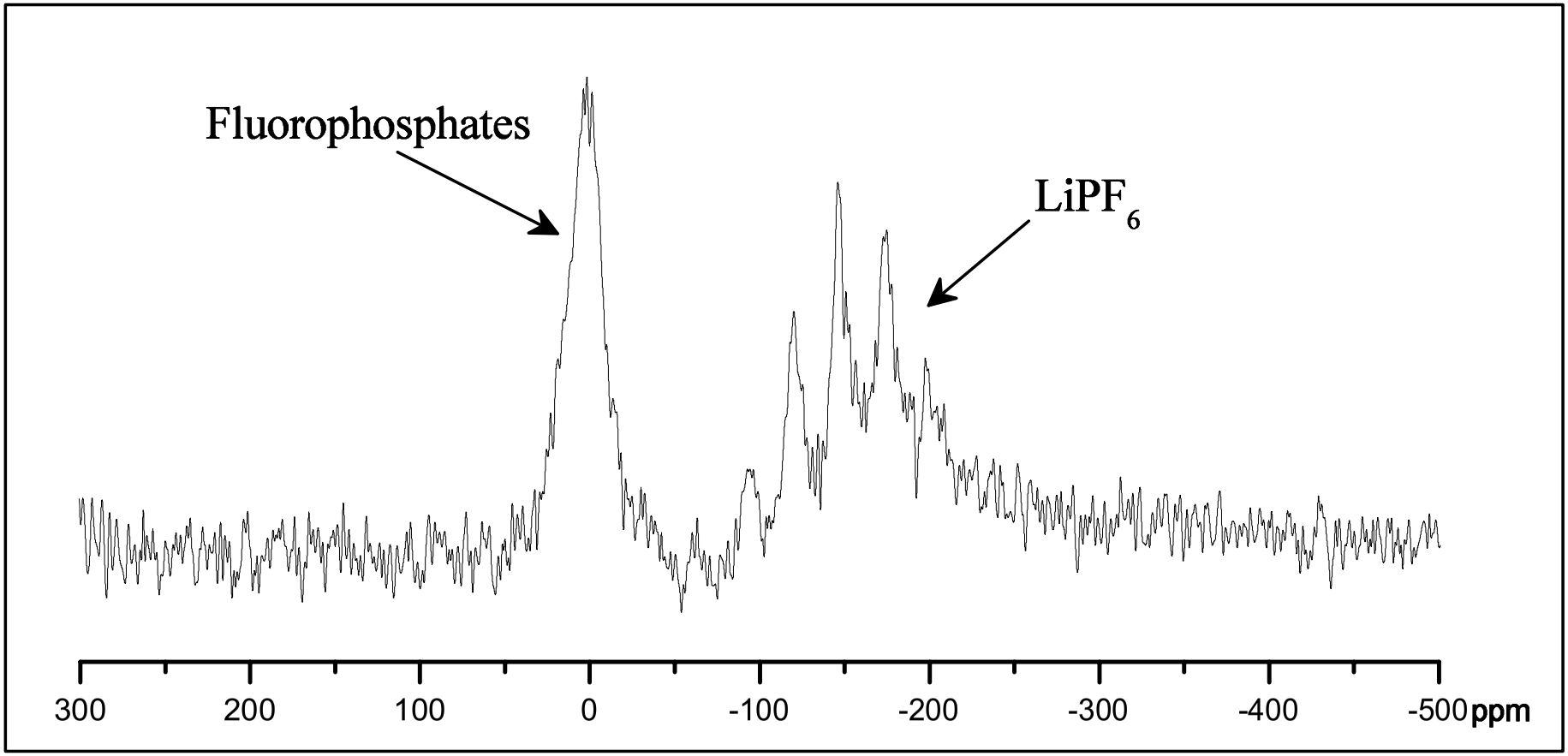
Fluorophosphates
LiPF6
300
200
100
0
-100
-200
-300
-400
-500
ppm

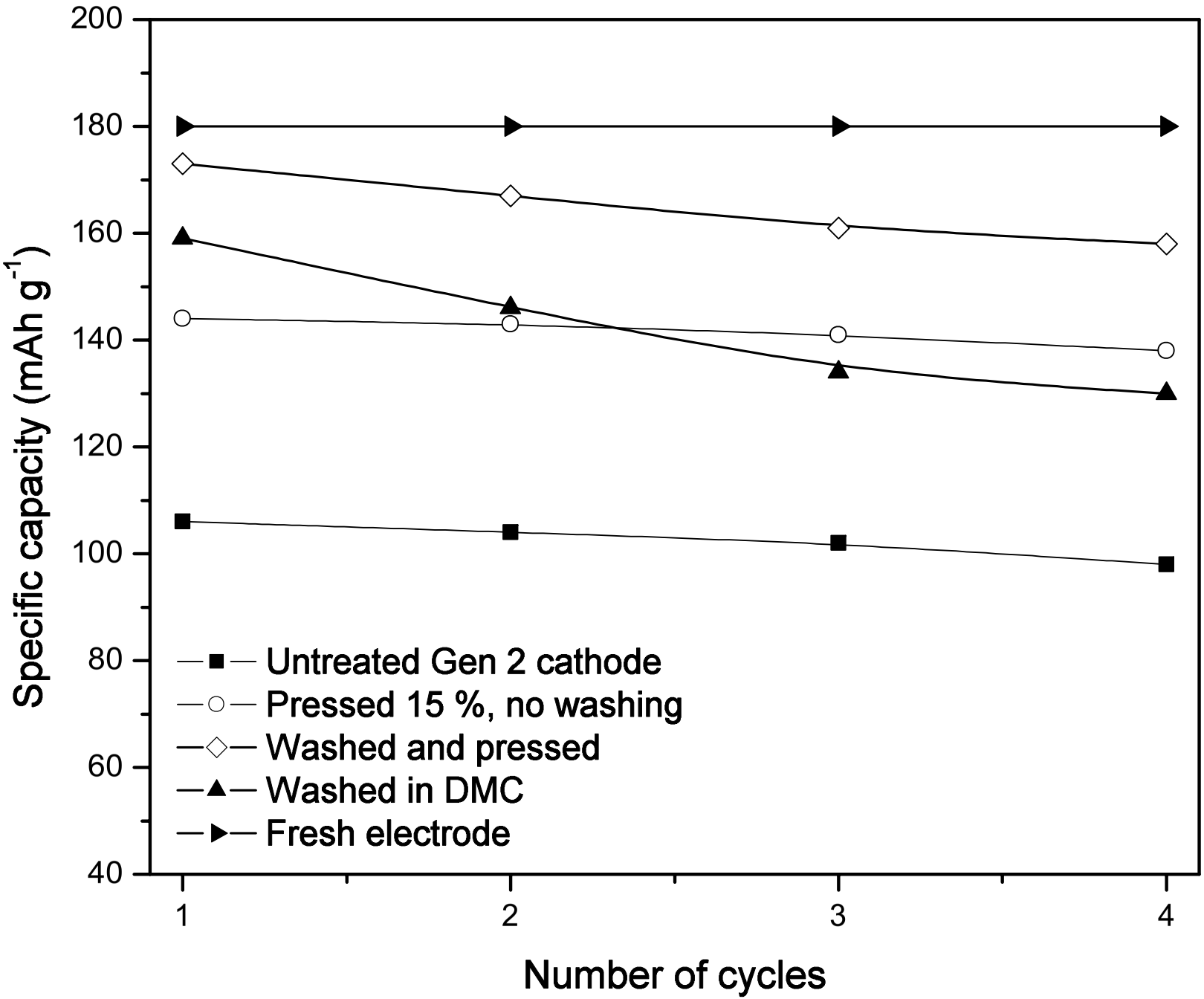
200
180
160
140
120
100
80
60
40
Specific capacity (mAh g-1)
1
2
3
4
Number of cycles
Untreated Gen 2 cathode
Pressed 15 %, no washing
Washed and pressed
Washed in DMC
Fresh electrode

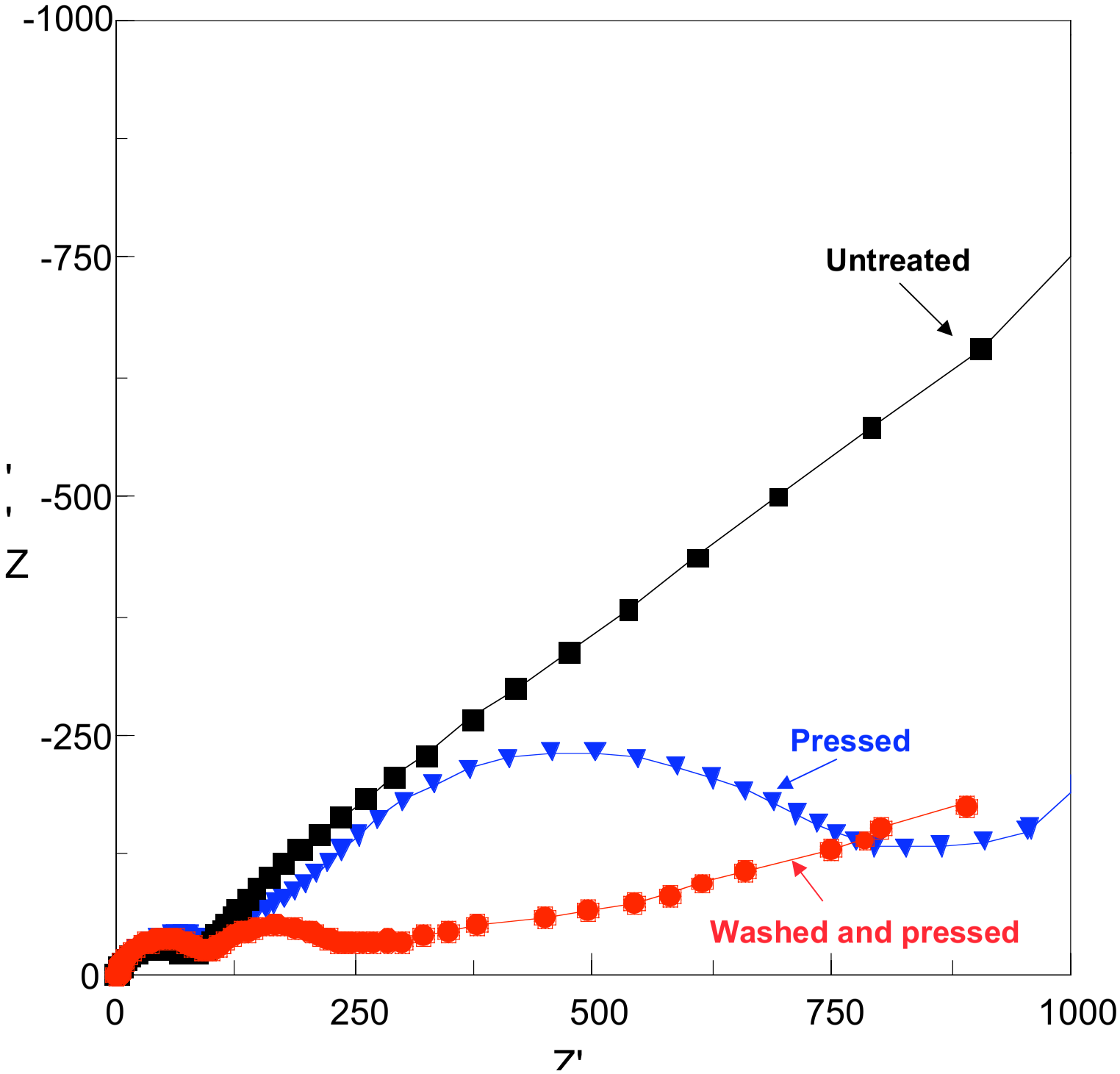
-1000
-750
-500
-250
0
Z'
0
250
500
750
1000
Z'
Untreated
Pressed
Washed and pressed

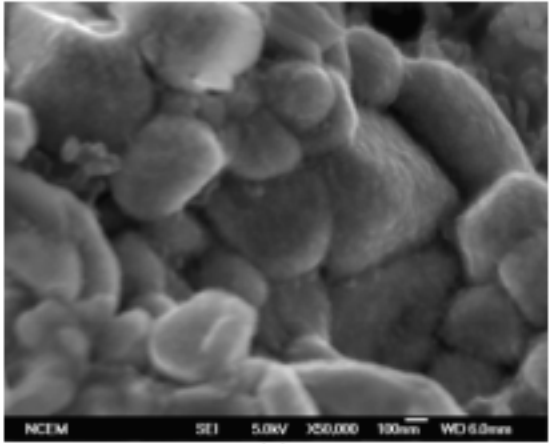
NCEM SEI 5.0kV X50,000 100nm WD 6.0mm

(a)

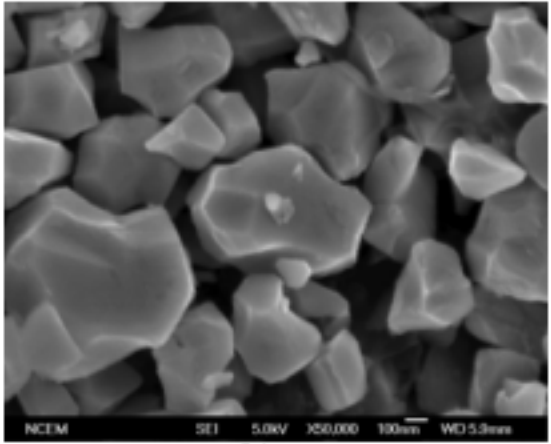
NCEM SEI 5.0kV X50,000 100nm WD 5.3mm

(b)